



Ceria and copper/ceria functional coatings for electrochemical applications: Materials preparation and characterization

J. Melnik^a, X.Z. Fu^a, J.L. Luo^{a,*}, A.R. Sanger^a, K.T. Chuang^a, Q.M. Yang^b

^a Department of Chemical and Materials Engineering, University of Alberta, Edmonton, Alberta T6G 2G6, Canada

^b Vale-Inco Technical Services Ltd., Mississauga, Ontario L5K 1Z9, Canada

ARTICLE INFO

Article history:

Received 6 October 2009

Received in revised form 27 October 2009

Accepted 27 October 2009

Available online 6 November 2009

Keywords:

Electrodeposition
Coating
Ceramics
Composite
Fuel cell

ABSTRACT

Following preliminary investigations, two electrodeposition techniques (electrophoretic and electrolytic) were selected and adapted for deposition of doped ceria ceramic and copper/doped ceria composite coatings on Ni substrates (foil and foam). The copper/doped ceria composites have potential value as protective functional coatings for current collectors in electrochemical cells including solid oxide fuel cells (SOFC). The doped ceria ceramic coating has potential application as a porous matrix for anodes of SOFCs operating on syngas, sour gas, or hydrocarbons.

© 2009 Elsevier B.V. All rights reserved.

1. Introduction

New, efficient, protective coatings for components in electrochemical cells are developed to address the specific needs of each application. Commonly, technical problems need to be addressed. It becomes challenging when the coating has to combine additional useful properties besides the protective function. Particularly, this is the key problem in materials science in development of coatings for high temperature chemical reactors and fuel cell power generators (solid oxide fuel cells: SOFCs) involving diverse catalytic and electrochemical processes. Depending on fuel composition or chemical reagents, type of chemical process, temperature, pressure, etc. the coatings for structural parts of such devices (catalytic reaction substrates, electrolytes, electrodes, current collectors, interconnects, etc.) must combine physical strength, durability, high chemical and thermal stability, catalytic activity, good ionic and/or electronic conduction, and, of course, physical compatibility with the substrate material. It happens very often that the means to address some of these requirements are conflicting or even incompatible, forcing us to look for compromise solutions. Ceramic functional layers and coatings for metals are among such problematical materials.

There is extensive technical and scientific literature concerning coating of metals with layers (films) of functional ceramics, as

advanced hi-tech industries need a wide range of new functional coatings with various useful properties, particularly for SOFCs and chemical reactors. The present research is directed specifically to development of SOFCs operating on syngas. Syngas is an economically promising feed for fuel cells since it is readily obtained from primary energy sources such as coal, coke or natural gas [1,2]. Pure Ni metal and some Ni-based alloys (Inconel, Incoloy, Hastelloy, Monel, etc.), as well as high nickel cast iron and chromium–molybdenum alloy steels, have been under extensive investigation as promising materials for use as current collectors and interconnects in hydrogen fueled SOFCs because they have excellent electric conductivity and enhanced resistance to redox corrosion. However, their direct use in fuels containing CO and H₂S gases (syngas, sour gas, hydrocarbons, etc.) is impractical as these components are aggressively corrosive and highly poisonous to Ni-based anode catalysts and current collectors. Therefore, to use these metals their surfaces and, specifically, the area in contact with the electrode must be modified and protected with functional coatings to provide high chemical resistance and physical durability, while retaining good electronic conductivity. Moreover, these coatings have to be physically compatible with the substrate metal(s). It is also desirable that they possess capability to catalyze anodic electrochemical processes, or are suitable for deposition of such catalysts. The material must provide good electrochemical connectivity between the current collector and the anode electrode, and may even substitute the coating material for the anode catalyst.

Among the limited number of types of potential materials possessing the required combination of properties are metal–ceramic

* Corresponding author. Tel.: +1 780 492 2232; fax: +1 780 492 2881.
E-mail address: jingli.luo@ualberta.ca (J.L. Luo).

composites (cermets) based on acceptor doped zirconia and ceria. Gadolinium or samarium doped ceria (GDC, SDC) have enhanced electronic conduction compared to doped zirconia, good catalytic activity for anodic oxidation reactions, are tolerant to carbon deposition and sulfurization, and require relatively low sintering temperatures [3,4].

Cu metal has excellent electronic conductivity and good carbon deposition tolerance, as well as acceptable resistance to small amounts (hundreds of ppm) of H₂S in reducing atmosphere of syngas [5,6].

Therefore, we selected GDC and Cu as promising components of functional composite coatings for syngas fueled SOFCs. We selected pure Ni metal as the primary substrate and, particularly, Ni foam which is popularly used as current collectors in commercial galvanic elements, and is a promising multifunctional component of the complex anodic compartment of SOFCs [7,8], but which is prone to attack by components of sour feeds.

Herein we present and discuss preparation of pure ceramic and metal–ceramic composite coatings by electrodeposition. Based on review of the literature and our preliminary experimental data, two electrodeposition methods were selected as they offer advantages when compared to alternative techniques as being more suitable for complex shaped components of state of the art SOFCs.

2. Experimental

2.1. Techniques and materials

Two deposition techniques were used to fabricate ceria ceramic and copper/ceria composite coatings onto Ni foil/foam substrates: cathodic electrophoretic deposition (EPD) from ceramic suspensions, and electrolytic deposition (ELD) from solutions of corresponding metal salts. A conventional electrolytic bath setup with vertical position of electrodes (flat sheets of metals) was used to deposit coatings on both sides of a cathode substrate placed between two anodes (impacts of variables are described in Section 3). A GAMRY electrochemical measurement system and Hewlett-Packard 740B DC standard/differential voltmeter were used as DC power sources.

Ni foil from Alfa Aesar (0.127 mm thick) and Ni foam sheets from Vale Inco (1.7 mm thick, 0.51 g cm⁻²) were used as cathode substrates. Platinum (0.127 mm thick) or copper (0.675 mm thick) foils from Alfa Aesar were used as anodes. Nanopowder of gadolinium doped ceria Ce_{0.8}Gd_{0.2}O_{1.9} (GDC) from NexTech Materials, copper(II) sulfate pentahydrate CuSO₄·5H₂O and cerium(III) nitrate hexahydrate Ce(NO₃)₃·6H₂O both from Alfa Aesar were used for preparation of suspensions and electrolyte solutions respectively. Poly vinyl butyral-co-vinyl alcohol-co-vinyl acetate (PVB) from Aldrich and butoxyethyl acid phosphate (BAP) from Yohoku Chemical Co., Ltd. were used as a binder and dispersant, respectively.

2.2. Measurements

The weight of deposits was determined gravimetrically after drying in air at 95 °C to constant weight. Density and porosity of deposits were calculated from the mass and volume.

Scanning electron microscopy (SEM) and energy-dispersive X-ray analysis (EDX) were used as the most potent and reliable methods to determine microstructure of surfaces and elemental composition of polished cross-sections of deposits. A Hitachi S-2700 scanning electron microscope equipped for energy-dispersive X-ray analysis was used.

DC electrical conductivity measurements were performed using the van der Pauw technique to measure the lateral conductivity of thin films, using a ProboStat A-6 and a Solartron SI 1287 electrochemical interface system.

3. Results and discussion

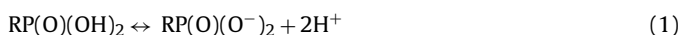
3.1. Electrolytic deposition of pure ceria and electrophoretic deposition of GDC

Electrodeposition methods were used as they can form uniform coatings on different (metal and nonmetal) substrates of complex shapes. Moreover, deposition rate, consequent thickness and uniformity of coating films can be rigidly controlled using applied electric field characteristics. Two electrodeposition techniques were used for ceramic coatings: electrophoretic deposition (EPD) and electrolytic deposition (ELD) [9,10]. Both techniques use a cathodic electrodeposition process. They differ in the nature of the starting materials: suspensions of ceramic powders, and solutions of corresponding metal salts, respectively. The former allows formation of thick ceramic coatings and compound bodies while the latter enables the formation of very thin ceramic films.

However, the major problem restricting application of these methods is incompatibility of ceramic coatings and metal substrates. Different mechanical (strength), physical (density, microstructure) and thermal (volume and phase changes) properties lead to crack formation, and subsequent peeling, after one or both of drying and heating of materials having ELD films [11–14]. While EPD coatings can be produced without cracks, they form bulk porous microstructures determined by ceramic particles size and shape [10,15]. The same problems arose when depositing ceria films by EPD (from 50 gL⁻¹ ceria suspension at 60V) and ELD (from 0.1 M Ce(NO₃)₃ solution at 1 mA cm⁻²) onto Ni foil substrates (Fig. 1). Typically, the EPD coatings (Fig. 1a) were loose and porous (porosity of about 40 vol.% calculated by mass and volume of deposits after drying), while the ELD coatings (Fig. 1b and c) had a lot of fractal cracks. The latter are a characteristic of coatings from very fine powders undergoing physical and chemical changes under drying (dehumidification) and heating (dehydration, phase transformations, volume changing) on physically different and incompatible substrates. Based on the preliminary EPD results, since there were significantly less structural defects, two significant advantages were found: controlled stoichiometry of deposits from the as-prepared gadolinium doped ceria powders (GDC), and control over a wide range of coating thickness (from a few to hundreds of microns) by controlling the deposition rate. Thus it was reasonable to improve the EPD methodology for applications with the present materials.

Two major problems were encountered: instability of suspensions to aggregation and sedimentation and, again, low compactness of dry deposits. As an electrochemical colloidal process, EPD requires both a stable colloid suspension of charged particles to provide their continuous motion under dc electric field (electrophoresis) and very efficient discharging and coagulation mechanisms to obtain a dense deposit. In attempts to overcome these contradictory limitations, various compositions of suspensions containing different organic binders, stabilizers, and dispersants were investigated [10,15–17]. Several dispersants/stabilizers and binders were experimentally tested for formation of ceria EPD coatings. Phosphate esters (PE) and polyvinyl butyral (PVB) were identified as the most efficient dispersant/stabilizer and binder respectively.

Phosphate esters are usually long-chain phosphate esters of ethoxylated alcohols: R_nP(O)(OH)_{3-n}, where R_n is (C₄H₉OC₂H₄O)_n (n = 1, 2) for butoxyethyl acid phosphate (BAP). It easily dissociates in ethanol solvent, liberating protons from the hydroxyl groups bonded to the phosphorus, and quickly reaches the equilibrium state (Eq. (1)) at concentrations about 1 wt.% [17]:



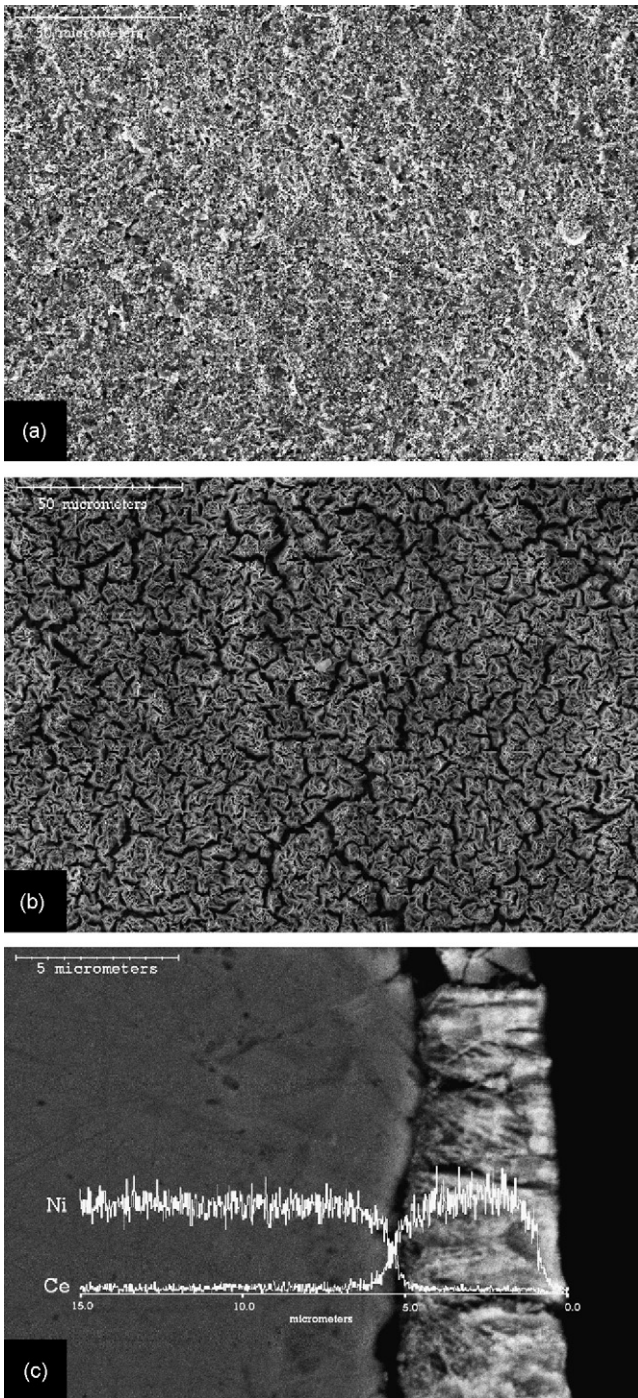


Fig. 1. SEM images of ceria coatings on the Ni foil substrate after heating at 900 °C in reducing atmosphere: (a) EPD and (b and c) ELD techniques. Image (c) is a cross-section view. EDX scanning lines of Ni and Ce are plotted on the image (c). Scale bars: 50 μm (a and b) and 5 μm (c).

Then, in the ethanol suspension of GDC, the protons adsorb on the surface hydroxyl groups of ceria particles according to acid–base interactions resulting in positively charged colloid particles (Eq. (2)):



This charging mechanism leads to dual potential benefits: effective stabilization of particles against aggregation, and efficient mass transfer of the dispersed ceria particles in the suspension. In our sedimentation tests we achieved visible stabilization of ethanol

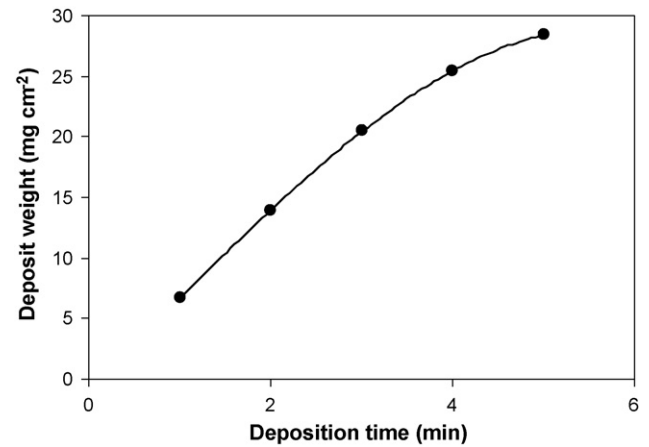


Fig. 2. Deposit weight vs. deposition time for the electrophoretic deposits obtained from 50 g L⁻¹ suspension of GDC nanopowder in ethanol.

suspensions containing up to 50 g L⁻¹ of GDC nanopowder for several hours when just 1 g L⁻¹ of BAP was added. The stabilization time was more than sufficient for application of the EPD procedures which usually lasted less than 1 h. The small amount of BAP required (much less than 1 wt.%) for successful stabilization of the suspension is attributable to catalyzation of dissociation of PE by the powder surface [18].

PVB is widely used as an effective binder in ceramics manufacture, and so it was selected in efforts to enhance densification of GDC deposits and to enhance their capability to adhere to the substrate. PVB is a copolymer of polyvinyl alcohol functional groups which readily adhere to hydroxyl groups on the particle surface and anchor PVB molecules to ceramic particles, and butyral groups which enhance suspension of particles bound to the co-polymer, thus enabling steric stabilization of ceramic suspensions. The most effective concentration range of PVB in GDC–ethanol suspensions was found to be 1–2 g L⁻¹. Bridging flocculation of the GDC powder occurred at greater concentrations of PVB. Further, at high concentrations the deposition rates decreased, ascribed to competitive adsorption of PVB and BAP resulting in decreased particle charge.

Suspension concentration and terminal voltage (or current) are the key parameters during operation of an EPD process, and these were optimized experimentally for the present GDC–ethanol suspensions and electrophoretic cell design. The maximum deposition rates were reached at constant voltage of about 75 V in suspensions containing 50 g L⁻¹ of GDC nanopowder, 1 g L⁻¹ of BAP and 2 g L⁻¹ of PVB. The deposits obtained under these EPD conditions were of highest quality. The deposited weight was exponentially related to time (Fig. 2), as there was a continuous drop of current (at constant voltage) due to the increased resistance with thickness of the deposited layer (ca. 50 μm after 5 min). The calculated porosity of the dry deposit was about 20 vol.%, a value comparable to green ceramic bodies prepared by regular mechanical compaction. Importantly, after drying the deposited layer had a uniform microglobular structure comprised of microflocules of deposited nanoparticles, without cracks and other visible defects. However, some voids and pores about 10 μm and less appeared after heating at 900 °C (Fig. 3a). The surface of the heated deposit still had microglobular structure (mostly < 20 μm). Thus it appears that the voids and pores probably arose from burn out of locally concentrated organic matter in addition to shrinkage of the particle aggregates. The presence of microaggregates in the deposited coatings could be indicative of sub-optimal mass ratios of BAP to PVB and (BAP + PVB) to ceramic powder. The relatively high voltage also may have affected the dispersion/coagulation mechanism. The

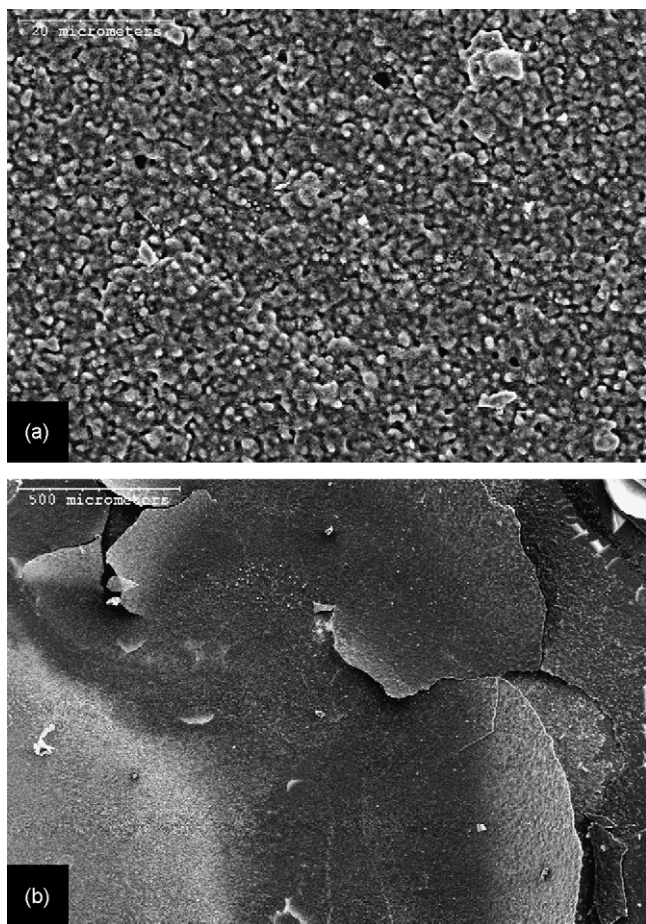


Fig. 3. SEM images of GDC coatings electrophoretically deposited onto Ni foil substrate from ethanol suspensions of nanosized GDC powder: (a) after heating at 900 °C and (b) after sintering at 1450 °C. Scale bars: 20 µm (a) and 500 µm (b).

data to date show that further research is required to optimize the EPD technique for application with the present materials.

Further, visible delamination occurred when the coated samples were sintered at high temperature (1450 °C). This was an expected effect for the initial samples, due to mismatch of thermal volume changes of the substrate and the deposit. Nevertheless, the initial adherence to the substrate was strong enough to leave an underlayer of the deposited material strongly adhered to the metal surface (Fig. 3b). This effect is not expected to occur in the desired process, as treatment at such high temperatures is not necessary for electrophoretically deposited ceramic coatings intended for much lower fuel cell application temperatures.

To summarize progress to date: we have shown that the EPD methodology is very promising for development of new, efficient, catalytically active, porous anodic matrixes supported with metal current collectors for SOFC applications. However, although advances have been achieved in application of EPD methods for deposition of GDC ceramic coatings on metal substrates, further improvements are required before their industrial implementation for manufacturing dense and durable protective functional coatings.

3.2. Electrodeposition of Cu/GDC coatings

The major purpose of many investigations into new metal–ceramic composites is improvement of traditional properties of coatings such as hardness, wear resistance, or corrosion resistance. There is extensive literature on development of

methods for deposition of composite metal–ceramic coatings. Several reports are pertinent to the present research directed to electrodeposition of Cu/GDC composites, in particular those describing Ni-based composite coatings containing CeO₂ [19–22], and Cu-based coatings containing CeO₂ [23], ZrO₂ [24], TiO₂ [25], and Al₂O₃ [26]. One of the main processing advantages of these coatings is the ability to apply them as prepared, without prior heat treatment. In general, composite coatings containing ceria nanoparticles had much higher corrosion resistance and durability through grain refinement strengthening than the pure coating metal. However, recent strong interest in the electrodeposition of functional metal–ceramic composite coatings (either dense or porous) for high temperature fuel cells application has appeared and is rapidly growing [8,21,27–32]. It should be noted that Cu/ceria composites have a combination of high electronic conduction and reasonable catalytic activity, and so are very promising materials for use as anodes in SOFCs operating with syngas or hydrocarbons as feed [33–35]. Particularly, a Cu anode containing about 30 vol.% of SDC (samaria doped ceria) showed good performance in SOFCs fed with hydrocarbons [31].

Here, Cu and GDC nanoparticles were co-electrodeposited onto Ni foil or Ni foam at room temperature in an electrolytic bath containing an aqueous acidic solution of copper sulfate and a suspension of GDC nanopowder. Concentrations of GDC nanopowder, CuSO₄·5H₂O, and H₂SO₄, current density, and cell configurations (area of electrodes and distance between them) were systematically varied to determine the optimum deposition rate and physical properties of the final coatings (composition and microstructure). The current density and GDC concentration in suspensions were the most significant variables, limiting the doped ceria content in the final deposits. It also was found that agitation of suspensions had a noticeable influence on the composition of deposits. The optimal stirring rate and the optimal position of the stirring bar depended on the cell configuration, since the stagnant zone in the cell usually was between the electrodes. A recent report describes ultrasonically assisted electrodeposition of Co/CeO₂ to avoid this problem [21]. However, the general applicability of this technique is as yet unproven, and so requires testing for the present application.

Summarizing the obtained experimental results, the following are most favorable conditions for the Cu/GDC electrodeposition: suspension composition, 200 g L⁻¹ of CuSO₄·5H₂O, 50 g L⁻¹ of H₂SO₄, and 50–200 g L⁻¹ of GDC nanopowder; cell configuration, working area of electrodes 2 cm² at a separation of 1.5 cm; processing conditions, 600–1000 rpm stirring rate (magnetic stirrer), 10–40 mA cm⁻² current density. A deposition time of 60 min is required to obtain thickness of deposits of tens of microns at 25 °C.

The current density and GDC concentration were the most significant parameters limiting the amount of GDC imbedded into the copper matrix. Therefore, these parameters were systematically varied in subsequent experiments (Fig. 4). The suspension concentration strongly affected the amount of GDC in copper deposits as determined using EDX analysis applied to polished cross-sections of coated Ni foil samples (Fig. 5). Increasing GDC concentration from 50 g L⁻¹ to 200 g L⁻¹ caused a substantial increase in GDC content, from 5 vol.% to 20 vol.%. However, it should be noted that it was difficult to maintain stability of very thick consistencies of suspensions (>150 g L⁻¹) during the deposition process due to strong tendency to aggregate and form sediment. As a result, the coatings obtained using high GDC concentrations had disorganized copper matrix structure and irregular distribution of GDC particles and aggregates in deposits (Fig. 5b). Increasing the stirring rate did not help because of strong turbulence in the bath at rates >1000 rpm. Use of organic stabilizers was limited by their water solubility and necessity of tolerance to the acid medium and copper cations. Therefore, although organic reagents were successfully used for electrophoretic deposition (as described above),

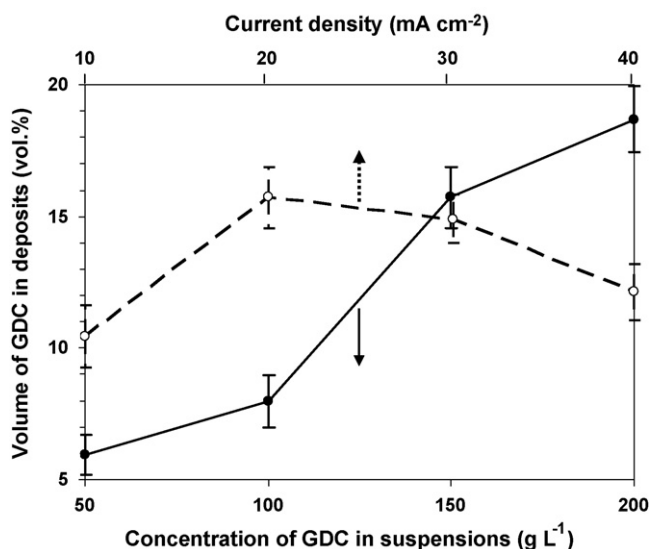


Fig. 4. Relationship between amount of GDC imbedded into Cu matrix (deposited onto Ni foil) and concentration of GDC nanopowder in suspensions at 20 mA cm⁻² current applied (solid line) or applied current density at concentration of 150 g L⁻¹ (stroked line). Experimental deviations, including measurement errors, are shown as vertical bars.

they were not effective for electrodeposition of composites. The best results achieved to date were for suspension concentrations of about 100–150 g L⁻¹. Nevertheless, it appears that a higher content of ceria in copper deposits can be achieved without structural disorganization by selecting proper stabilizers and dispersing agents.

The amount of GDC in composite deposits was between 10 vol.% and 15 vol.% at current densities in the range 10–40 mA cm⁻² using

150 g L⁻¹ suspension concentration, and had a pronounced maximum at 20 mA cm⁻². A similarly extreme trend was observed for other suspension concentrations. The increase of the GDC content with increasing current was expected considering mobility of charged particles, but its decrease at current higher than 20 mA cm⁻² was unexpected, and may have occurred as a result of electrolysis of components and/or recharging of particles. The maximum amount of GDC nanoparticles imbedded into copper matrix was about 20 vol.% at 20 mA cm⁻² and a ceria concentration of 200 g L⁻¹. The thickness of the deposited coatings was in the range from 30 μm to 50 μm.

3.3. Structural and electrical characterization of composite coatings

Microstructures and compositions of electrodeposited Cu/GDC coatings on Ni foil and foam were determined using SEM–EDX analysis (Figs. 5–7). As previously mentioned, composite deposits having 5–12 vol.% of GDC (by EDX) obtained from suspensions with <150 g L⁻¹ GDC (optimally 100 g L⁻¹) had strong and dense well organized microstructures of the Cu metal matrix (Fig. 5a). Uniformly distributed ceramic nanoparticles were tightly imbedded between copper grains in the matrix (Fig. 6c). In contrast, use of very concentrated suspensions (at least 150–200 g L⁻¹) led to strongly disorganized microstructure of the metal matrix (Fig. 5b) with clearly defined aggregates of ceramic particles, however the overall deposits were compact and without visible cracks or contiguous pores or channels. Comparing deposits formed by pure copper and Cu/GDC composites (Fig. 6b and 6c), it was found that presence of ceramic nanoparticles significantly decreased the size of copper crystallites, similar to effects reported for comparable composites [19,20,22,24]. The composite coatings deposited onto Ni foil were strong and dense, and similar results were obtained for Cu/GDC deposits on Ni foam (Fig. 7).

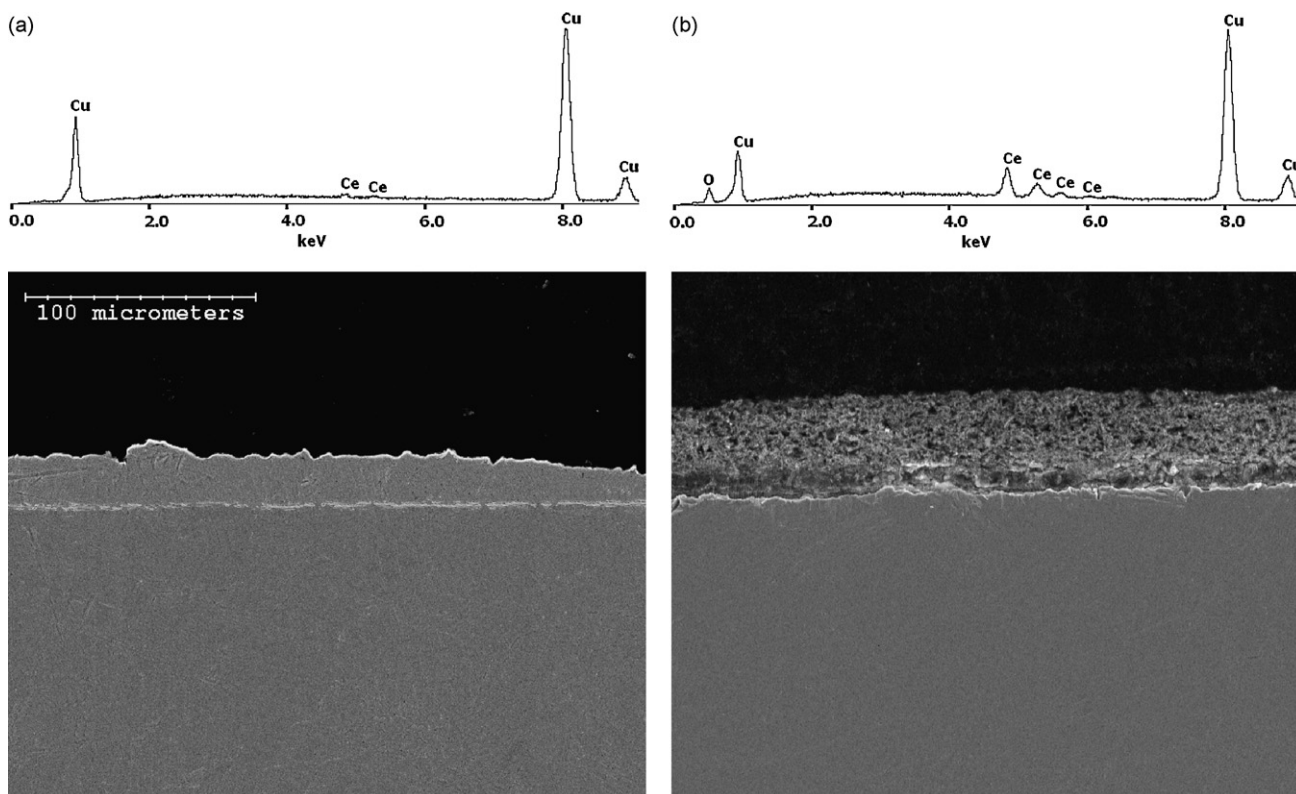


Fig. 5. Cross-sectional SEM images and EDX patterns of Cu/GDC deposits: (a) 5 vol.% and (b) 20 vol.% of GDC. Scale bar: 100 μm.

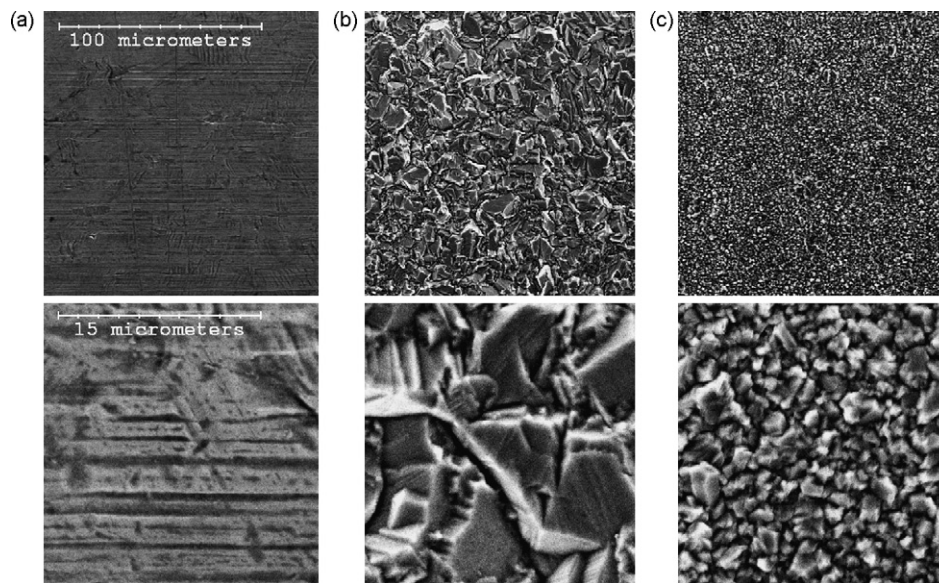


Fig. 6. SEM images of coatings deposited onto Ni foil: (a) pure Ni foil substrate; (b) pure copper deposit; (c) Cu/SDC composite (~9 vol.% of Cu). Scale bars: 100 μm (upper images) and 15 μm (lower images).

A series of electric conductivity tests was carried out to determine the effects of the presence of ceramics on electronic conduction of the Cu/GDC composite coatings at low and high temperatures. It was expected that ceramic particles located between copper crystallites would significantly affect total electric conductivity of regular polycrystalline Cu metal. The van der Pauw technique was chosen as the most reliable method to measure the lateral conductivity of thin flat coatings deposited onto Ni foil. It should be noted that for clearer evaluation of the conductivity of thin films a substrate should have significantly lower conduction and greater thickness. In our case, the pure Ni metal substrate had conductivity about 4 times lower than that of pure Cu metal at room

temperature and about 7 times lower in the range 300–600 °C (CRC Handbook). The thickness of the substrate was about 3–4 times greater than that of coatings (127 μm vs. 30–40 μm). These circumstances allowed us to measure the samples' conductivity as a whole, as well as to evaluate the influence of ceramics on their lateral conductivity. The conductivity data obtained at room temperature (about 20 °C) in air and 600 °C in a reducing atmosphere (to prevent metal oxidation) for different coating compositions deposited onto Ni foil are summarized in [Table 1](#).

As expected, the electric conductivity was inversely proportional to the amount of the doped ceria in the composites. At both 20 °C and 600 °C, a minor but evident and almost linear drop of

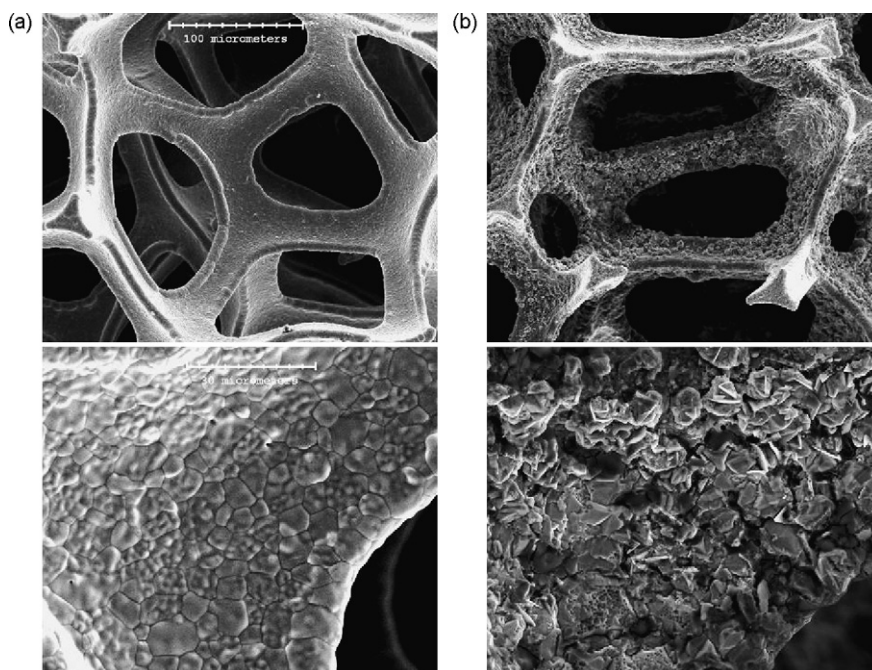


Fig. 7. SEM images of coatings deposited onto Ni foam: (a) pure Ni foam substrate and (b) Cu/SDC composite (~9 vol.% of Cu). Scale bars: 100 μm (upper images) and 30 μm (lower images).

Table 1
Electrical conductivities ($10^5 \Omega^{-1} \text{cm}^{-1}$) of Cu/GDC coatings of different compositions.

Temperature ($^{\circ}\text{C}$)	GDC content in Cu/GDC coatings (vol.%)				
	0	5	9	12	20
20	5.96	5.77	5.54	5.27	3.80
600	1.70	1.65	1.50	1.46	1.04

conductivity (11–14% in total) was observed for coatings deposited from suspensions of concentrations less than 150 g L^{-1} . However, conductivity of composite coatings contained about 20 vol.% GDC (deposited from very thick suspensions) dropped more noticeably (36–39%) due to the above mentioned specific microstructure and so-called “the composite effect” (uneven transition from quantity to quality). Nevertheless, in spite of the changes observed, the absolute values of measured electrical conductivities are very high and more than enough for conductivity requirements for current collectors or electrodes of fuel cells.

4. Conclusions

Based on literature survey and our preliminary experiments, two electrodeposition techniques (electrophoretic and electrolytic) were selected, adapted and improved for preparation of ceria ceramic and copper/ceria composite coatings on Ni substrates (foil and foam), for potential use as protecting functional coatings for current collectors and electrodes in SOFC fueled with syngas, sour gas, or hydrocarbons. Theoretical and practical improvements have been developed to enable better control of the preparation of deposits having designated properties. The pure ceramic coatings prepared from gadolinium doped ceria had porosity about 20 vol.% and formed structures which can be used as a porous matrix for SOFC composite anodes. For the first time, Cu/GDC composite coatings with higher content of ceramics in the Cu matrix (about 15 vol.%) were prepared using electrodeposition, and their microstructure and electric conductivity were characterized. The composite coatings did not need heat treatment, appeared to be sufficiently dense (microscopically) for the proposed application, and had high electrical conductivity comparable to that of Cu metal. Therefore these materials are good prospects for use as protective functional coatings for current collectors of SOFC. Further research presently underway includes detailed studies of protective and electrochemical characteristics, as well as SOFC performance tests with syngas.

Acknowledgement

This work is supported by Natural Sciences and Engineering Research Council of Canada/INCO CRD Grant.

References

- [1] Z.R. Xu, J.L. Luo, K.T. Chuang, A.R. Sanger, *J. Phys. Chem. C* 111 (2007) 16679–16685.
- [2] J.H. Wu, Y.T. Fang, Y. Wang, D.K. Zhang, *Energy Fuels* 19 (2005) 512–516.
- [3] H. Lin, C. Ding, K. Sato, Y. Tsutai, H. Ohtaki, M. Iguchi, C. Wada, T. Hashida, *Mater. Sci. Eng. B* 148 (2008) 73–76.
- [4] M. Gong, X. Liu, J. Tremblay, C. Johnson, *J. Power Sources* 168 (2007) 289–298.
- [5] H. He, R.J. Gorte, J.M. Vohs, *Electrochem. Solid-State Lett.* 8 (2005) A279–A280.
- [6] O.C. Nunes, R.J. Gorte, J.M. Vohs, *J. Power Sources* 141 (2005) 241–249.
- [7] Q.M. Yang, V.A. Ettel, J. Babjak, D.K. Charles, M.A. Mosoiu, *J. Electrochem. Soc.* 150 (2003) A543–A550.
- [8] S.F. Corbin, R.M.C. Clemmer, Q. Yang, *J. Am. Ceram. Soc.* 92 (2) (2009) 331–337.
- [9] P. Sarkar, P.S. Nicholson, *J. Am. Ceram. Soc.* 79 (8) (1996) 1987–2002.
- [10] I. Zhitomirsky, A. Petric, *J. Eur. Ceram. Soc.* 20 (2000) 2055–2061.
- [11] I. Zhitomirsky, A. Petric, *Mater. Lett.* 40 (1999) 263–268.
- [12] T.D. Golden, A.Q. Wang, *J. Electrochem. Soc.* 150 (9) (2003) C621–C624.
- [13] R.N. Bhattacharya, S. Phok, *Phys. Stat. Sol. (a)* 203 (15) (2006) 3734–3742.
- [14] E.A. Kulp, S.J. Limmer, E.W. Bohannon, J.A. Switzer, *Solid State Ionics* 178 (2007) 749–757.
- [15] I. Zhitomirsky, A. Petric, *Ceram. Int.* 27 (2001) 149–155.
- [16] F. Tang, T. Uchikoshi, K. Ozawa, Y. Sakka, *J. Eur. Ceram. Soc.* 26 (2006) 1555–1560.
- [17] T. Uchikoshi, Y. Sakka, *J. Am. Ceram. Soc.* 91 (6) (2008) 1923–1926.
- [18] I. Zhitomirsky, A. Petric, *J. Mater. Sci.* 39 (2004) 825–831.
- [19] N.S. Qu, D. Zhu, K.C. Chan, *Scripta Mater.* 54 (2006) 1421–1425.
- [20] Y.-J. Xue, X.-Z. Jia, Y.-W. Zhou, W. Ma, J.-S. Li, *Surf. Coat. Technol.* 200 (2006) 5677–5681.
- [21] C. Argirusis, S. Matic, O. Schneider, *Phys. Stat. Sol. (a)* 205 (10) (2008) 2400–2404.
- [22] Y. Zhou, H. Zhang, *Xiyou Jinshu Cailiao Yu Gongcheng* 37 (3) (2008) 448–451.
- [23] O. Mitoseriu, C. Iticescu, G. Carac, *Rev. Chim.* 55 (7) (2004) 525–529.
- [24] L. Benea, O. Mitoseriu, J. Galland, F. Wenger, P. Ponthiaux, *Mater. Corros.* 51 (2004) 491–495.
- [25] N. Guglielmi, *J. Electrochem. Soc.* 119 (8) (1972) 1009–1012.
- [26] J.P. Celis, J.R. Roos, *J. Electrochem. Soc.* 124 (10) (1977) 1508–1511.
- [27] N. Shaigan, D.G. Ivey, W. Chen, *J. Electrochem. Soc.* 155 (4) (2008) D278–D284.
- [28] P. Sarkar, L. Yamarte, H. Rho, L. Johanson, *Int. J. Appl. Ceram. Technol.* 4 (2) (2007) 103–108.
- [29] I. Krkljus, Z. Brankovic, K. Duris, V. Vukotic, G. Brankovic, S. Bernik, *Int. J. Appl. Ceram. Technol.* 5 (6) (2008) 548–556.
- [30] M. Zunic, L. Chevallier, F. Deganello, A. D'Epifanio, S. Licocchia, E. Di Bartolomeo, E. Traversa, *J. Power Sources* 190 (2009) 417–422.
- [31] S. Jung, M.D. Gross, R.J. Gorte, J.M. Vohs, *J. Electrochem. Soc.* 153 (8) (2006) A1539–A1543.
- [32] S. Jung, J.M. Vohs, R.J. Gorte, *J. Electrochem. Soc.* 154 (12) (2007) B1270–B1275.
- [33] C. Lu, W.L. Worrell, J.M. Vohs, R.J. Gorte, *J. Electrochem. Soc.* 150 (10) (2003) A1357–A1359.
- [34] A.C. Tavares, B.L. Kuzin, S.M. Beresnev, N.M. Bogdanovich, E.K. Kurumchin, Y.A. Dubitsky, A. Zaopo, *J. Power Sources* 183 (2008) 20–25.
- [35] X.-F. Ye, B. Huang, S.R. Wang, Z.R. Wang, L. Xiong, T.L. Wen, *J. Power Sources* 164 (2007) 203–209.